PROCEEDINGS OF THE
AMERICAN MATHEMATICAL SOCIETY
Volume 137, Number 9, September 2009, Pages 3077–3090
S 0002-9939(09)09852-9
Article electronically published on March 18, 2009

QUADRATIC RATIONAL MAPS LACKING PERIOD 2 ORBITS

RIKA HAGIHARA

(Communicated by Jane M. Hawkins)

ABSTRACT. We study dynamical properties of a parameterized family of quadratic rational maps, all of whose members lack period 2 orbits. We classify regions in the parameter space of the family according to the behavior of marked critical points. We characterize the parameter space by comparing it with the Mandelbrot set.

1. INTRODUCTION

In the theory of iteration of rational maps, periodic points play important roles. Every rational map has infinitely many periodic points (Beardon [2]); however, some rational maps fail to have periodic points of a certain period. Baker [1] proved that if a polynomial P of degree at least 2 has no periodic points of period n, then $n = 2$ and P is conformally conjugate to $z \mapsto z^2 - z$. As for rational maps, he proved the following.

Theorem 1.1 ([1])**.** *Let R be a rational map of degree d, where $d \geq 2$. If R has no periodic points of period n, then the pair (d, n) is either $(2, 2)$, $(2, 3)$, $(3, 2)$ or $(4, 2)$. Such R exists for each pair (d, n).*

Kisaka [9] listed all possible forms of such exceptional rational maps. The author [6] gave a complete proof of the classification.

The $(2, 2)$ case is conformally conjugate to the parameterized family of rational maps $R_a(z) = \frac{z^2-z}{az+1}$, where $a \in \mathbb{C} \setminus \{-1\}$. Recall that every quadratic rational map has two distinct critical points (Milnor [13]). Members of the family $\{R_a\}$ can be characterized as having a parabolic fixed point with multiplier -1 and one immediate basin. Hence for each parameter a one of the critical points of R_a must be associated to the parabolic fixed point. The main purpose of this paper is to demonstrate the existence of a unique critical point associated to this parabolic fixed point. Consequently, there is a "free" critical point. Since, depending on the parameter value a, the map R_a has an attracting cycle, we would expect to see a copy of the Mandelbrot set in the parameter space of $\{R_a\}$ arising from the bifurcation of this free critical point. The parameter space of $\{R_a\}$ in $[-3, 3] \times [-3i, 3i]$ is shown in Figure 1. A holomorphic copy of the figure appears in [13].

This paper is organized as follows. In Section 2 we collect preliminary results about R_a and use them to reduce the parameter space of $\{R_a\}$ by conjugacy.

Received by the editors October 23, 2008, and, in revised form, December 8, 2008.
2000 *Mathematics Subject Classification.* Primary 37F45; Secondary 30D05, 37F10.
Key words and phrases. Complex dynamics, parabolic, critical points.

©2009 American Mathematical Society
Reverts to public domain 28 years from publication

License or copyright restrictions may apply to redistribution; see https://www.ams.org/journal-terms-of-use

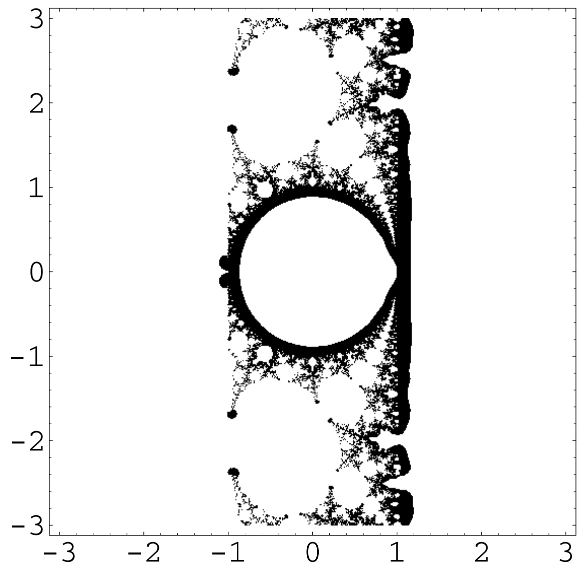

FIGURE 1. The parameter space of $\{R_a\}$.

In Section 3 we classify regions of the parameter space of $\{R_a\}$ according to the behavior of marked critical points. The main theorem asserts that we can specify a unique critical point associated to the parabolic fixed point of R_a. We further prove interesting dynamics that R_a exhibits for certain parameter values. In Section 4 we compare the characteristics of the Mandelbrot set and the parameter space of $\{R_a\}$. The computer algorithm used for producing the parameter space picture is explained in the Appendix.

Much work has been done on the dynamics of quadratic rational maps. Milnor [13, 14] and Rees [15] worked on the moduli space of quadratic rational maps quite generally. Specific slices of the moduli space have also been studied by Hawkins [7] and Milnor [13], with the latter work including parabolic ones. Results in this article provide proofs of some of the observations in [13].

This paper is based on the author's dissertation research at the University of North Carolina at Chapel Hill under the supervision of Dr. Jane Hawkins. Some computer programs used are edited versions of Maple and Mathematica programs first written by Dr. Lorelei Koss.

2. Reduction of the parameter space

We first reduce the parameter space of $\{R_a\}$ by conformal conjugacy and then identify points of the reduced parameter space by symmetry. We define the equivalence relation among parameters by $a \sim a'$ if and only if the corresponding maps R_a and $R_{a'}$ are conformally conjugate. With it we form a *reduced set* $\mathcal{R}_a$ by taking a representative from each equivalence class.

The fixed points of $R_a(z) = \frac{z^2-z}{az+1}$ are 0, ∞, and $\frac{2}{1-a}$ with multipliers -1, a, and $\frac{3-a}{1+a}$, respectively. Hence R_a and $R_{a'}$ are conformally conjugate if and only if $a' = a$ or $a' = \frac{3-a}{1+a}$ ([2]). Set $f(a) = \frac{3-a}{1+a}$.

License or copyright restrictions may apply to redistribution; see https://www.ams.org/journal-terms-of-use

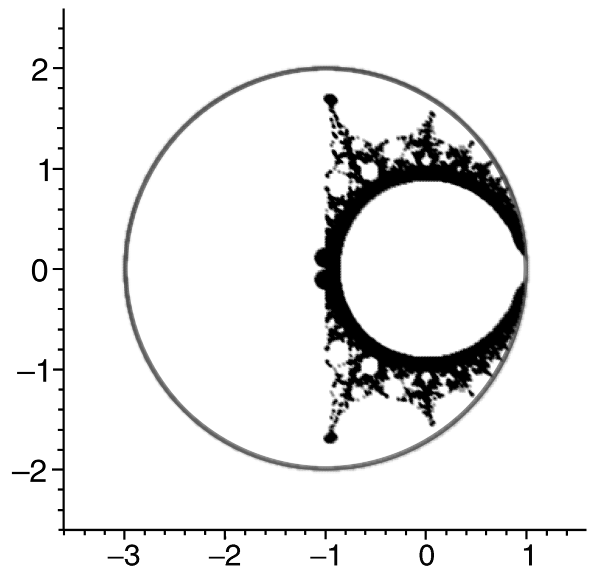

FIGURE 2. $\mathcal{R}_a$.

Lemma 2.1. *The map f satisfies the following.*

(i) $a \sim f(a)$.
(ii) *The inverse of f is itself.*
(iii) *The function f maps the circle $C = \{a \in \mathbb{C} : |a+1| = 2\}$ onto itself.*

Proof. The first two results follow from the definition of f (see [9]). For (iii) an easy calculation shows that $f(-1+2e^{i\theta}) = -1+2e^{-i\theta}$ for $\theta \in \mathbb{R}$. □

Theorem 2.2. *A reduced set $\mathcal{R}_a$ can be taken as*

$$\mathcal{R}_a = \{a \in \mathbb{C} : 0 < |a+1| < 2\} \cup \{a \in \mathbb{C} : |a+1| = 2,\, 0 \leq \mathrm{Im}(a)\}.$$

Proof. Note that $f : \{a \in \mathbb{C} : 0 < |a+1| < 2\} \to \{a \in \mathbb{C} : 2 < |a+1|\}$ is a bijection. The proof of Lemma 2.1 shows that complex conjugates on $C = \{a \in \mathbb{C} : |a+1| = 2\}$ can be identified with each other. □

The set $\mathcal{R}_a$ is in the reduced form under conformal conjugacy. It is the region inside and the upper half of the circle in Figure 2. Next, we identify points of $\mathcal{R}_a$ using symmetry.

Lemma 2.3. *For $\varphi(z) = \bar{z}$, we have $\varphi \circ R_{\bar{a}} \circ \varphi^{-1} = R_a$.*

This implies that although R_a and $R_{\bar{a}}$ are not conformally conjugate, their dynamics are symmetric about the real line, and thus the reduced set $\mathcal{R}_a$ has symmetry about the real line. Therefore, it suffices to use parameters in

$$\mathcal{R}_a^{\mathrm{sym}} = \{a \in \mathbb{C} : 0 < |a+1| \leq 2,\, 0 \leq \mathrm{Im}(a)\}$$

to study how the dynamics of R_a depend on the parameter a.

License or copyright restrictions may apply to redistribution; see https://www.ams.org/journal-terms-of-use

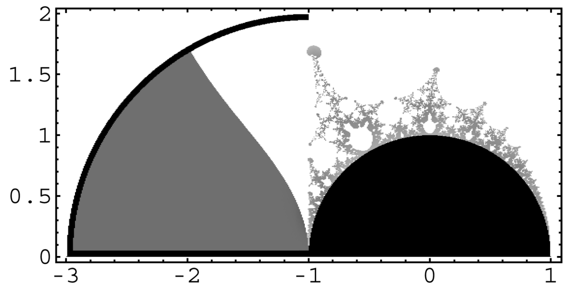

FIGURE 3. A_1, A_2, A_3, and A_4 in $\mathcal{R}_a^{\text{sym}}$.

3. THE ROLES OF CRITICAL POINTS

Each map $R_a(z) = \frac{z^2-z}{az+1}$ has two distinct critical points. By construction R_a has a parabolic fixed point 0 with one immediate basin consisting of two disjoint Fatou components. Hence for each parameter a one of the critical points of R_a must be associated to 0. Theorem 3.1 asserts that for much of the reduced set $\mathcal{R}_a$ a unique critical point is associated to 0.

Theorem 3.1. *The orbit of the critical point* $c_1 = \frac{-1+\sqrt{1+a}}{a}$ *of* R_a *converges to the parabolic fixed point* 0 *for each parameter* a *in the following sets:*

$$A_1 = \{a \in \mathcal{R}_a : |a| < 1\};$$
$$A_2 = \{a \in \mathcal{R}_a : -3 \leq a < -1\};$$
$$A_3 = \{a \in \mathcal{R}_a : \operatorname{Re}(a + \tfrac{4}{a+1}) < -3\};$$
$$A_4 = \{a \in \mathcal{R}_a : |a+1| = 2,\ -3 \leq \operatorname{Re}(a) < -1\}.$$

For parameters in A_1*, the orbit of the critical point* $c_2 = \frac{-1-\sqrt{1+a}}{a}$ *converges to the attracting fixed point* ∞*. For parameters in* A_2*,* A_3*, and* A_4*, the orbits of both critical points* c_1 *and* c_2 *converge to* 0*. For parameters in* A_4*, the orbits of both critical points lie on the circle of center* $\frac{2}{1-a}$ *(another fixed point of* R_a*) and radius* $|\frac{2}{1-a}|$*.*

The parameters in $\mathcal{R}_a^{\text{sym}}$ for which Theorem 3.1 holds are colored black (sets A_1, A_2, A_4) and gray (A_3) in Figure 3. The proof is divided into cases which are proved as separate results.

Case 1. $A_1 = \{a \in \mathcal{R}_a : |a| < 1\}$. We use the following theorem.

Theorem 3.2 ([11])**.** *Let* f_λ *be a holomorphic family of rational maps parameterized by a connected complex manifold* Λ*, and let* x *be a point in* Λ*. Suppose that* $c_i : \Lambda \to \widehat{\mathbb{C}}$ *are holomorphic maps parameterizing the critical points of* f_λ*. Then the following conditions are equivalent.*

(i) *The number of attracting cycles of* f_λ *is locally constant at* x*.*
(ii) *For each* i*, the functions* $\lambda \mapsto {f_\lambda}^n(c_i(\lambda))$*,* $n = 0, 1, 2, \ldots$*, form a normal family at* x*.*

Proof for Case 1. For a parameter a in $A_1 = \mathbb{D}$, R_a has an attracting fixed point ∞ with multiplier a and a parabolic fixed point 0. Since R_a has two critical points

License or copyright restrictions may apply to redistribution; see https://www.ams.org/journal-terms-of-use

c_1 and c_2, Theorem 3.2 implies that for each i the family $\{(R_a)^n(c_i)\}_{n=0}^{\infty}$ converges normally at a to either 0 or ∞. For $a = 0$ the critical point c_2 itself is a superattracting fixed point ∞. Hence for each $a \in A_1$ the critical point c_1 is associated to 0, and c_2 to ∞. □

Case 2. $A_2 = \{a \in \mathcal{R}_a : -3 \le a < -1\}$.

Proof. The critical points c_1 and c_2 of R_a are complex conjugates, and so are their corresponding iterates under R_a. Hence the orbits of both critical points converge to the parabolic fixed point 0. □

Case 3. $A_3 = \{a \in \mathcal{R}_a : \mathrm{Re}(a + \frac{4}{a+1}) < -3\}$. We use results of Bergweiler [3] and Buff and Epstein [5] on the number of critical points in the immediate basins of a parabolic fixed point.

Lemma 3.3 ([3], [5])**.** *Let R be a rational map having a fixed point α with multiplier $e^{2\pi i \frac{p}{q}}$. Then there exists an integer $k \ge 1$ called the* parabolic multiplicity *of α and a local holomorphic coordinate φ defined near α such that $\varphi(\alpha) = 0$ and*

$$(\varphi \circ R \circ \varphi^{-1})(z) = e^{2\pi i \frac{p}{q}} z(1 + z^{qk} + \beta z^{2qk}) + \mathrm{O}(|z|^{2qk+2}).$$

A holomorphic change of coordinates leaves β invariant.

Define the *résidu iteratif* of R at α by $\mathrm{résit}(R, \alpha) = \frac{qk+1}{2} - \beta$.

Theorem 3.4 ([3], [5])**.** *Let R be a rational map having a fixed point α with multiplier $e^{2\pi i \frac{p}{q}}$ and parabolic multiplicity k. If the union of the immediate basins of α contains exactly k simple critical points of R, then* $\mathrm{Re}(\mathrm{résit}\,(R^q, \alpha)) \ge \frac{qk}{4}$*. In particular, when* $\mathrm{Re}(\mathrm{résit}\,(R^q, \alpha)) < \frac{qk}{4}$*, the union of the immediate basins of α contains at least $k+1$ critical points of R, counting multiplicity.*

Proof for Case 3. In the setting of ${R_a}^2$ we have $\alpha = 0$, $p = q = 1$, and $k = 2$. Write $a = \lambda e^{i\theta} - 1$, where $0 < \lambda \le 2$ and $\frac{\pi}{2} < \theta \le \pi$. Conjugate ${R_a}^2$ first by $\varphi_1(z) = i\sqrt{2\lambda} e^{i\frac{\theta}{2}} z$ and then by $\varphi_2(z) = z(1 + \frac{i\sqrt{\lambda} e^{i\frac{\theta}{2}}}{2\sqrt{2}} z)$ so that

$$((\varphi_2 \circ \varphi_1) \circ ({R_a}^2) \circ (\varphi_2 \circ \varphi_1)^{-1})(z) = z + z^3 + \tfrac{1}{8}(5 - a - \tfrac{4}{a+1}) z^5 + \mathrm{O}(z^6).$$

Hence $\beta = \frac{1}{8}(5 - a - \frac{4}{a+1})$ for ${R_a}^2$ and

$$\mathrm{résit}\,({R_a}^2, 0) = \tfrac{1 \cdot 2 + 1}{2} - \tfrac{1}{8}(5 - a - \tfrac{4}{a+1}) = \tfrac{1}{8}(7 + a + \tfrac{4}{a+1}).$$

For R_a we have $\alpha = 0$, $p = 1$, $q = 2$, and $k = 1$. The second part of Theorem 3.4 implies that when $\mathrm{Re}(\mathrm{résit}({R_a}^2, 0)) < \frac{2 \cdot 1}{4} = \frac{1}{2}$, the immediate basin of the parabolic fixed point 0 contains both critical points c_1 and c_2. This happens when $\mathrm{Re}(\mathrm{résit}({R_a}^2, 0)) = \mathrm{Re}(\frac{1}{8}(7 + a + \frac{4}{a+1})) < \frac{1}{2}$, i.e. when $\mathrm{Re}(a + \frac{4}{a+1}) < -3$. □

Case 4. $A_4 = \{a \in \mathcal{R}_a : |a+1| = 2,\ -3 \le \mathrm{Re}(a) < -1\}$. The main steps of the proof are as follows. We first show that both critical points c_1 and c_2 as well as the fixed point 0 of R_a lie on the circle C_θ in $\mathbb{C}$ of center $\frac{2}{1-a}$ (another fixed point of R_a). This circle is shown to be forward invariant under R_a. We next consider the relative location of the critical points and some of their iterative images under R_a. We then form on C_θ a simple path from each critical point to 0. With the information on the location of key points, we proceed to show that the successive images of the paths under R_a shrink to 0. We now provide the details of the proof.

License or copyright restrictions may apply to redistribution; see https://www.ams.org/journal-terms-of-use

We first prove a result on the location of c_1 and c_2 in a more general setting. For a parameter a in $\mathcal{R}_a^{\text{sym}} = \{a \in \mathbb{C} : 0 < |a+1| \leq 2,\, 0 \leq \text{Im}(a)\}$, write $a = \lambda e^{i\theta} - 1$, where $0 < \lambda \leq 2$ and $0 \leq \theta \leq \pi$. With this notation the critical points of R_a are $c_1 = \frac{1}{1+\sqrt{\lambda}e^{i\frac{\theta}{2}}}$ and $c_2 = \frac{1}{1-\sqrt{\lambda}e^{i\frac{\theta}{2}}}$. Define a circle C_θ in $\mathbb{C}$ as having center $c = \frac{1}{1-e^{i\theta}}$ and radius $|c|$, so that C_θ passes through the fixed point 0 of R_a.

Proposition 3.5. *For every $a = \lambda e^{i\theta} - 1$, where $0 < \lambda \leq 2$ and $0 < \theta \leq \pi$, both critical points c_1 and c_2 of R_a lie on C_θ.*

Proof. Using the trigonometric expressions for the center $c = \frac{1}{2} + \frac{i}{2} \cdot \frac{\cos\frac{\theta}{2}}{\sin\frac{\theta}{2}}$ of C_θ and the critical point $c_1 = \frac{\cos\frac{\theta}{2} + \frac{1}{\sqrt{\lambda}} - i\sin\frac{\theta}{2}}{\frac{\lambda+1}{\sqrt{\lambda}} + 2\cos\frac{\theta}{2}}$ of R_a, we calculate that $|c|^2 = |c - c_1|^2 = \frac{1}{4\sin^2\frac{\theta}{2}}$. A calculation for c_2 is similar. □

Corollary 3.6. *In the setting of Proposition* 3.5*, we have* $\text{Re}(c) = \frac{1}{2}$ *and* $C_\theta \cap \mathbb{R} = \{0, 1\}$*.*

Proof. The circle C_θ has a center whose real coordinate is $\frac{1}{2}$, and C_θ passes through 0. By symmetry C_θ intersects with the real axis at 1. Indeed, the point 1 is a pre-image of 0. □

Remarks 3.7. When $\theta = 0$, the point $c = \frac{1}{1-e^{i\theta}}$ is ∞ and the critical points c_1 and c_2 have real values. Hence c, c_1, and c_2 can be viewed as lying on the "extended" circle $C_{\mathbb{R}} = \{z \in \mathbb{R}\} \cup \{\infty\}$ in $\widehat{\mathbb{C}}$.

Next, we restrict to parameters on a part of the semi-circular boundary of $\mathcal{R}_a^{\text{sym}}$.

Lemma 3.8. *For every $a = 2e^{i\theta} - 1$, where $0 < \theta \leq \pi$, the following hold.*

(i) *The center c of C_θ coincides with the fixed point $\frac{2}{1-a}$ of R_a.*

(ii) *The circle C_θ is forward invariant under R_a.*

Proof. When $\lambda = 2$ (so that $|a+1| = 2$) and $\theta \neq 0$ ($a \neq 1$), an easy calculation shows that the center $\frac{1}{1-e^{i\theta}}$ of C_θ coincides with the fixed point $\frac{2}{1-a}$ of R_a and that C_θ has radius $|c| = \frac{-ie^{\frac{i\theta}{2}}}{1-e^{i\theta}}$. Write an arbitrary point p on C_θ as

$$p = \frac{1}{1-e^{i\theta}} + \frac{-ie^{\frac{i\theta}{2}}}{1-e^{i\theta}} \cdot e^{i\alpha},$$

where $\alpha \in \mathbb{R}$. Then

$$R_a(p) = -\frac{(i + e^{\frac{i}{2}(2\alpha+\theta)})(e^{\frac{i\theta}{2}} - ie^{i\alpha})}{(-1+e^{i\theta})(-e^{i\alpha} + ie^{\frac{i\theta}{2}} + 2e^{i(\alpha+\theta)})}.$$

We need to check the distance between $R_a(p)$ and the center c of C_θ:

$$R_a(p) - c = \frac{e^{i\alpha}(e^{i\theta} + ie^{\frac{i}{2}(2\alpha+\theta)} - 2)}{(-1+e^{i\theta})(-e^{i\alpha} + ie^{\frac{i\theta}{2}} + 2e^{i(\alpha+\theta)})}.$$

In order to see that $R_a(p) - c$ has modulus $|c| = \frac{1}{|1-e^{i\theta}|}$, we multiply $R_a(p) - c$ by $-e^{-i(\alpha+\theta)}$ of unit modulus and obtain

$$\frac{e^{i\alpha}(-e^{-i\alpha} - ie^{-\frac{i\theta}{2}} + 2e^{-i(\alpha+\theta)})}{(-1+e^{i\theta})(-e^{i\alpha} + ie^{\frac{i\theta}{2}} + 2e^{i(\alpha+\theta)})}.$$

License or copyright restrictions may apply to redistribution; see https://www.ams.org/journal-terms-of-use

The factors $-e^{-i\alpha} - ie^{-\frac{i\theta}{2}} + 2e^{-i(\alpha+\theta)}$ in the numerator and $-e^{i\alpha} + ie^{\frac{i\theta}{2}} + 2e^{i(\alpha+\theta)}$ in the denominator are complex conjugates. Since $\alpha \in \mathbb{R}$, the difference $R_a(p) - c$ has modulus $|\frac{e^{i\alpha}}{-1+e^{i\theta}}| = \frac{1}{|1-e^{i\theta}|}$. Therefore, a point on the circle C_θ is mapped to a point on the same circle. $\square$

For the rest of this section we restrict our attention to A_4 and assume that $a = 2e^{i\theta} - 1$, where $\frac{\pi}{2} < \theta \leq \pi$. Let ℓ denote the line in $\mathbb{C}$ that passes through 0 and the center c of the circle C_θ. Then ℓ splits C_θ into two halves. Let ℓ' be the tangent line to C_θ at 0.

When $\theta = \pi$, the circle C_θ has center $\frac{1}{2}$ and radius $\frac{1}{2}$. So ℓ is the real axis and ℓ' the imaginary axis in $\mathbb{C}$: in fact, $\ell \cup \{\infty\} = J$ (Proposition 3.18) and ℓ' is the axis of petals at 0. The critical point c_1 and the image $R_a(c_2)$ of c_2 are on C_θ and on the same side along ℓ, while c_2 and $R_a(c_1)$ are on C_θ and on the other side.

Note that c, c_1, c_2, $R_a(c_1)$, and $R_a(c_2)$ move continuously with respect to θ. We use the notation $c_1(\theta)$, for example, to emphasize that c_1 is a continuous function of θ. The next lemma shows that for $\theta \in (\frac{\pi}{2}, \pi)$, c_1 and $R_a(c_2)$ stay on one side along ℓ, while c_2 and $R_a(c_1)$ remain on the other.

Lemma 3.9. *For $\theta \in (\frac{\pi}{2}, \pi)$, the following hold.*

(i) *Both $|c_1|$ and $|R_a(c_1)|$ are neither the diameter of the circle C_θ nor 0.*
(ii) *Both $|c_2|$ and $|R_a(c_2)|$ are neither the diameter of the circle C_θ nor 0.*

Proof. (i) For $c_1 = \frac{1}{1+\sqrt{2}e^{i\frac{\theta}{2}}}$, we have $|c_1|^2 = |c_1|^2(\theta) = \frac{1}{3+2\sqrt{2}\cos\frac{\theta}{2}}$, so $|c_1|^2$ and hence $|c_1|$ are monotone increasing on $(\frac{\pi}{2}, \pi)$. As for the diameter of C_θ, it is $2|c| = \frac{1}{\sin\frac{\theta}{2}}$, which is monotone decreasing on $(\frac{\pi}{2}, \pi)$. We see that $|c_1|$ and $2|c|$ satisfy the inequality $0 < \frac{1}{\sqrt{5}} = |c_1|(\frac{\pi}{2}) < |c_1|(\pi) = \frac{1}{\sqrt{3}} < 1 = 2|c|(\pi)$. Thus $|c_1|$ is neither the diameter of C_θ nor 0 for $\theta \in (\frac{\pi}{2}, \pi)$. For $R_a(c_1) = \frac{-1}{(1+\sqrt{2}e^{i\frac{\theta}{2}})^2} = -{c_1}^2$, the above inequality implies that $|R_a(c_1)|$ satisfies the claim.

(ii) For $c_2 = \frac{1}{1-\sqrt{2}e^{i\frac{\theta}{2}}}$, we have $|c_2|^2 = \frac{1}{3-2\sqrt{2}\cos\frac{\theta}{2}}$, so $|c_2|^2$ and hence $|c_2|$ are monotone decreasing on $(\frac{\pi}{2}, \pi)$. Note that the inequality $0 < \frac{1}{\sqrt{3}} = |c_2|(\pi) < |c_2|(\frac{\pi}{2}) = 1 = 2|c|(\pi)$ holds. As for $R_a(c_2) = \frac{-1}{(1-\sqrt{2}e^{i\frac{\theta}{2}})^2} = -{c_2}^2$, we have $0 < \frac{1}{3} = |R_a(c_2)|(\pi) < |R_a(c_2)|(\frac{\pi}{2}) = 1 = 2|c|(\pi)$. Hence both $|c_2|$ and $|R_a(c_2)|$ are neither $2|c|$ nor 0 for $\theta \in (\frac{\pi}{2}, \pi)$. $\square$

Remarks 3.10. The proof of Lemma 3.9 in particular shows that $0 < |c_1| < 1 < 2|c|$, $0 < |c_2| < 1$, and $0 < |R_a(c_2)| < 1$ for $\theta \in (\frac{\pi}{2}, \pi)$.

The following two lemmas compare the moduli of the critical points and some iterative images of c_1 under R_a.

Lemma 3.11. *The inequality $|R_a(c_1)| < |c_2|$ holds for $\theta \in (\frac{\pi}{2}, \pi)$.*

Proof. We have $|R_a(c_1)| = \frac{1}{3+2\sqrt{2}\cos\frac{\theta}{2}}$ and $|c_2|^2 = \frac{1}{3-2\sqrt{2}\cos\frac{\theta}{2}}$. Hence for $\theta \in (\frac{\pi}{2}, \pi)$ the inequality $0 < |R_a(c_1)| < |c_2|^2$ holds. Since $0 < |c_2| < 1$ by Remarks 3.10, it must be that $0 < |R_a(c_1)| < |c_2|$ for $\theta \in (\frac{\pi}{2}, \pi)$. $\square$

Lemma 3.12. *The inequality $|{R_a}^2(c_1)| < |c_1|$ holds for $\theta \in \left(\frac{\pi}{2}, \pi\right)$.*

License or copyright restrictions may apply to redistribution; see https://www.ams.org/journal-terms-of-use

Proof. With ${R_a}^2(c_1) = \frac{1+\sqrt{2}e^{i\frac{\theta}{2}}+e^{i\theta}}{(1+\sqrt{2}e^{i\frac{\theta}{2}})^3}$ we calculate

$$|c_1| - |{R_a}^2(c_1)| = \frac{2|e^{i\theta} + \sqrt{2}e^{i\frac{\theta}{2}} + \frac{1}{2}| - |1 + \sqrt{2}e^{i\frac{\theta}{2}} + e^{i\theta}|}{|1 + \sqrt{2}e^{i\frac{\theta}{2}}|^3}.$$

Set $F(\theta) = 2|e^{i\theta} + \sqrt{2}e^{i\frac{\theta}{2}} + \frac{1}{2}| - |1 + \sqrt{2}e^{i\frac{\theta}{2}} + e^{i\theta}|$. Then

$$\begin{aligned} F(\theta) &\geq 2(|e^{i\theta} + \sqrt{2}e^{i\frac{\theta}{2}} + 1| - \tfrac{1}{2}) - |e^{i\theta} + \sqrt{2}e^{i\frac{\theta}{2}} + 1| \\ &= |e^{i\theta} + \sqrt{2}e^{i\frac{\theta}{2}} + 1| - 1 \\ &\geq |e^{i\frac{\theta}{2}} + \tfrac{\sqrt{2}}{2}|^2 - \tfrac{1}{2} - 1 = |e^{i\frac{\theta}{2}} + \tfrac{\sqrt{2}}{2}|^2 - \tfrac{3}{2}. \end{aligned}$$

Note that $|e^{i\frac{\theta}{2}} + \frac{\sqrt{2}}{2}|^2 = \frac{3}{2} + \sqrt{2}\cos\frac{\theta}{2} > \frac{3}{2}$ for $\theta \in (\frac{\pi}{2}, \pi)$. Hence $F > 0$ and thus $|c_1| - |{R_a}^2(c_1)| > 0$ for $\theta \in (\frac{\pi}{2}, \pi)$. □

So far we have shown that for each parameter value a in A_4 the fixed point 0 and the critical points c_1, c_2 of R_a lie on the forward invariant circle C_θ of center $\frac{2}{1-a}$. We have also checked the relative location and moduli of the critical points and some of their iterative images under R_a.

We now construct simple paths on C_θ from critical points c_i to 0 and show that their successive images under R_a shrink to 0. Cut C_θ at c_i and 0 and form two arcs on C_θ whose end points are c_i and 0. Denote by c_i0 the shorter of the two. Let $f_{c_i} : [0,1] \to C_\theta$ denote any simple path such that $f_{c_i}(0) = c_i$, $f_{c_i}(1) = 0$, and $f_{c_i}([0,1]) = c_i0$. Also, cut the circle C_θ into two halves by the line ℓ that passes through 0 and the center c of C_θ. Define C_θ^1 (C_θ^2, respectively) to be one of the halves that contains c_1 and $R_a(c_2)$ (c_2 and $R_a(c_1)$, respectively).

Lemma 3.13. *For $i = 1, 2$, the path $R_a \circ f_{c_i} : [0,1] \to C_\theta$ is a simple path from $R_a(c_i)$ to 0, and its image is $R_a(c_i)0$.*

Proof. We will prove the statement only for $i = 1$. The composite $R_a \circ f_{c_1}$ is a path from $[0,1]$ into C_θ with the initial point $(R_a \circ f_{c_1})(0) = R_a(c_1)$ and the final point $(R_a \circ f_{c_1})(1) = R_a(0) = 0$. In order to show that $R_a \circ f_{c_1}$ is a simple path, suppose that it is not. Then there exist α_1 and α_2 such that $0 \leq \alpha_1 < \alpha_2 \leq 1$ and $(R_a \circ f_{c_1})(\alpha_1) = (R_a \circ f_{c_1})(\alpha_2)$. Since $R_a \circ f_{c_1}$ is a continuous path with its image in C_θ, at least one of the following three subcases must occur.

Subcase 1. There exist β_1, β_2, β_3 satisfying either $0 \leq \beta_1 \leq \alpha_1 < \beta_2 < \beta_3 \leq \alpha_2 \leq 1$ or $0 \leq \alpha_1 \leq \beta_1 < \beta_2 < \alpha_2 \leq \beta_3 \leq 1$, and $(R_a \circ f_{c_1})(\beta_1) = (R_a \circ f_{c_1})(\beta_2) = (R_a \circ f_{c_1})(\beta_3)$. This is a contradiction, since R_a is of degree 2 and the pre-images of any point under R_a must consist of two points, counting multiplicity. (Here, we use the fact that the path f_{c_1} is simple.)

Subcase 2. For $0 = \alpha_1 < \alpha_2 < 1$ we have $(R_a \circ f_{c_1})(\alpha_1) = (R_a \circ f_{c_1})(\alpha_2) = R_a(c_1)$. Since c_1 is a critical point of R_a, the pre-images of $R_a(c_1)$ consist of c_1 with multiplicity 2. However, the above equation shows that $R_a(c_1)$ has three pre-images, c_1, c_1, and $f_{c_1}(\alpha_2) \neq c_1$, counting multiplicity.

Subcase 3. For $0 < \alpha_1 < \alpha_2 = 1$ we have $(R_a \circ f_{c_1})(\alpha_1) = (R_a \circ f_{c_1})(\alpha_2) = 0$. This is a contradiction, since then the pre-images of 0 under R_a are 0, 1, and $f_{c_1}(\alpha_1)$, the last of which is neither 0 nor 1 by Remarks 3.10.

License or copyright restrictions may apply to redistribution; see https://www.ams.org/journal-terms-of-use

Thus, $R_a \circ f_{c_1}$ is a simple path. Note that part of the image of f_{c_1}, $\{f_{c_1}(x) : 1-\epsilon < x < 1\}$ for small enough $\epsilon > 0$, is in C_θ^1 and is contained in a petal at 0. This portion is mapped by R_a to a Fatou component that contains the other petal at 0, so the image of this portion must lie on C_θ^2. Thus the image of the path $R_a \circ f_{c_1}$ must coincide with $R_a(c_1)0$. □

Similarly, by cutting the circle C_θ at c_i and 1, we form on C_θ two arcs whose end points are c_i and 1. Define c_i1 to be the arc that does not intersect with c_i0 except at c_i. Let $g_{c_i} : [0,1] \to \mathbb{C}$ denote any simple path such that $g_{c_i}(0) = c_i$, $g_{c_i}(1) = 1$, and $g_{c_i}([0,1]) = c_i1$. Techniques in the proof of Lemma 3.13 can be applied to obtain the following.

Lemma 3.14. *For $i = 1, 2$, the path $R_a \circ g_{c_i} : [0,1] \to C_\theta$ is a simple path from $R_a(c_i)$ to 0, and its image is $R_a(c_i)0$.*

Using these paths we now show that critical orbits converge to 0.

Proposition 3.15. *The orbit of c_1 converges to 0 for $\theta \in \left(\frac{\pi}{2}, \pi\right)$.*

Proof. The simple path f_{c_1} has image c_10. Lemma 3.13 states that the composite $R_a \circ f_{c_1}$ is a simple path with image $R_a(c_1)0$. Lemma 3.11 implies that $R_a(c_1)0 \subset c_20$. In turn, the simple path f_{c_2} has image c_20, and Lemma 3.13 states that the composite $R_a \circ f_{c_2}$ is a simple path with image $R_a(c_2)0$, which lies on C_θ^1. Hence $R_a(c_1)0$ must be mapped to ${R_a}^2(c_1)0$. Since $|{R_a}^2(c_1)| < |c_1|$ by Lemma 3.12, the inclusion ${R_a}^2(c_1)0 \subset c_10$ holds. Inductively, we obtain the following sequences:

$$\cdots \subset {R_a}^{2(n+1)}(c_1)0 \subset {R_a}^{2n}(c_1)0 \subset {R_a}^{2(n-1)}(c_1)0 \subset \cdots \subset {R_a}^2(c_1)0 \subset c_10;$$

$$\cdots \subset {R_a}^{2n+1}(c_1)0 \subset {R_a}^{2n-1}(c_1)0 \subset {R_a}^{2n-3}(c_1)0 \subset \cdots \subset R_a(c_1)0 \subset c_20.$$

From these we obtain two monotone decreasing sequences, $\{|{R_a}^{2n}(c_1)|\}$ and $\{|{R_a}^{2n-1}(c_1)|\}$. By Lemma 3.13 both sequences have only positive terms. The Monotone Sequence Theorem implies that both sequences converge. Suppose that $\lim_{n\to\infty} |{R_a}^{2n}(c_1)| = \alpha$. Since the points ${R_a}^{2n}(c_1)$ lie on c_10 and c_10 is contained in C_θ^1, which is half of a circle having 0 as one of its end points, c_10 and the circle of center 0 and radius α have only one intersection A. Then it must be $\lim_{n\to\infty} {R_a}^{2n}(c_1) = A$.

We claim that $\lim_{n\to\infty} {R_a}^{2n}(c_1) = 0$. To this end, note that from the continuity of R_a we have

$$A = \lim_{n\to\infty} {R_a}^{2(n+1)}(c_1) = {R_a}^2(\lim_{n\to\infty} {R_a}^{2n}(c_1)) = {R_a}^2(A).$$

Hence ${R_a}^2(A) = A$. Since ${R_a}^2$ fixes 0, ∞, and $\frac{2}{1-a}$, A must be one of these. Here, ∞ is inappropriate since A lies on the circle C_θ in $\mathbb{C}$. Also, $\frac{2}{1-a}$ is inappropriate since it is the center of C_θ. Thus, A must be 0. A similar argument shows that $\lim_{n\to\infty} {R_a}^{2n-1}(c_1) = 0$. This completes the proof of Proposition 3.15. □

Proposition 3.16. *The orbit of c_2 converges to 0 for $\theta \in (\frac{\pi}{2}, \pi)$.*

Proof. Unlike c_1, for which Lemma 3.11 showed that $|R_a(c_1)| < |c_2|$ holds for $\theta \in (\frac{\pi}{2}, \pi)$, a similar inequality for c_2 does not hold for all $\theta \in (\frac{\pi}{2}, \pi)$. Instead, when $\theta = \cos^{-1}(-\frac{3}{4})$, c_1 and $R_a(c_2)$ coincide, and depending on the value of θ we have either

(i) $|R_a(c_2)| < |c_1|$ for $\theta \in (\cos^{-1}(-\frac{3}{4}), \pi)$ or

License or copyright restrictions may apply to redistribution; see https://www.ams.org/journal-terms-of-use

(ii) $|R_a(c_2)| > |c_1|$ for $\theta \in (\frac{\pi}{2}, \cos^{-1}(-\frac{3}{4}))$.

For (i) an argument analogous to the one in Proposition 3.15 shows that the orbit of c_2 converges to 0. For (ii) we observe the following. For a simple path f_{c_2} from c_2 to 0 with image $c_2 0$, the composite $R_a \circ f_{c_2}$ is a simple path with image $R_a(c_2)0$ that contains c_1. Lemmas 3.13 and 3.14 with Remarks 3.10 imply that ${R_a}^2 \circ f_{c_2}$ is a concatenation of two simple paths, one from ${R_a}^2(c_2)$ to $R_a(c_1)$ and the other from $R_a(c_1)$ to 0. Using Lemma 3.11 we obtain

$${R_a}^2(c_2)0 \subset R_a(c_1)0 \subset c_2 0.$$

The composite $R_a \circ f_{c_2}$ is a simple path. This, coupled with the proof of Proposition 3.15 showing that ${R_a}^2(c_1)0 \subset c_1 0$, gives

$${R_a}^3(c_2)0 \subset {R_a}^2(c_1)0 \subset c_1 0.$$

By induction we obtain

$${R_a}^{n+1}(c_2)0 \subset {R_a}^n(c_1)0.$$

Since $\lim_{n\to\infty} {R_a}^n(c_1) = 0$, $\lim_{n\to\infty} {R_a}^n(c_2) = 0$ also. Lastly, for $\theta = \cos^{-1}(-\frac{3}{4})$ we have $|R_a(c_2)| = |c_1|$ and hence $R_a(c_2) = c_1$; thus both critical orbits converge to the parabolic fixed point 0. □

This completes the proof of Theorem 3.1.

We have additional results on the Fatou and Julia sets of R_a. For a rational map R on $\widehat{\mathbb{C}}$, the *Fatou set* $F(R)$ of R is the maximal open subset of $\widehat{\mathbb{C}}$ in which $\{R^n\}_{n\in\mathbb{N}}$ forms a normal family. The *Julia set* $J(R)$ is the complement of the Fatou set. The Fatou set F and the Julia set J are completely invariant under R: $R^{-1}(F) = F = R(F)$ and $R^{-1}(J) = J = R(J)$. Also, for any positive integer n, $F(R^n) = F(R)$ and $J(R^n) = J(R)$. If $\deg R \geq 2$, then $J(R)$ is a perfect set, and either $J = \widehat{\mathbb{C}}$ or J has empty interior ([2]). The following corollary is an easy consequence of Case 4.

Corollary 3.17. *For $a \in A_4$, points on $C_\theta \setminus \{0,1\}$ are in the Fatou set of R_a.*

For each a in A_2, we can show that the Julia set J of R_a is a Jordan curve. In fact, we have the following result.

Proposition 3.18. *For $a \in A_2$, $J(R_a) = C_{\mathbb{R}} = \{z \in \mathbb{R}\} \cup \{\infty\}$.*

Proof. The circle $C_{\mathbb{R}}$ is completely invariant under R_a. By the minimality of the Julia set, $C_{\mathbb{R}} \supset J$. The set J cannot be totally disconnected since R_a has a parabolic fixed point whose immediate basin consists of disjoint Fatou components. If $C_{\mathbb{R}} \neq J$, then both J and the closure of $C_{\mathbb{R}} \setminus J$ are infinite and completely invariant. However, this cannot happen by the minimality of J. □

4. Comparison with the Mandelbrot set

In this section we define and explain equivalent statements for the Mandelbrot set M. Using Theorem 3.1 we define a Mandelbrot-set-like object M' for $\{R_a\}$ and observe differences in dynamical properties between M and M' that the existence of a parabolic fixed point brings about. Let $P_c(z) = z^2 + c$. For all $c \in \mathbb{C}$, the quadratic polynomial P_c has a super-attracting fixed (hence critical) point ∞ and

License or copyright restrictions may apply to redistribution; see https://www.ams.org/journal-terms-of-use

one critical point 0 in $\mathbb{C}$. In the dynamical plane of P_c, the immediate basin A_∞ of ∞ is both forward and backward invariant under P_c; in particular, $A_\infty = \{z \in \widehat{\mathbb{C}} : {P_c}^n(z) \to \infty\}$. The complement $\widehat{\mathbb{C}} \setminus A_\infty = \{z \in \mathbb{C} : {P_c}^n(z) \nrightarrow \infty\}$ is bounded and hence compact. The boundary of A_∞ is the Julia set of P_c.

The parameter space of $\{P_c\}$ depicts the Mandelbrot set M. The Mandelbrot set has two, possibly three, equivalent characterizations.

Definition A. The Mandelbrot set M is defined by $M = \{c \in \mathbb{C} : {P_c}^n(0) \nrightarrow \infty\}$.

Proposition B. *The Mandelbrot set is the connectivity locus of $J(P_c)$.*

Conjecture C. *The Mandelbrot set is the closure of the hyperbolicity locus of P_c.*

Proposition D. *The Mandelbrot set is the "filled" bifurcation locus of $\{P_c\}$.*

Definition A means that the Mandelbrot set is the set of c-values for which the critical point 0 of P_c is not in A_∞ and hence the critical orbit is bounded.

Proposition B means that the Mandelbrot set M is equivalent to the set of c-values for which the Julia set of $P_c = z^2 + c$ is connected. This equivalence goes back to Fatou and Julia (see e.g. Branner [4]). Fatou and Julia proved that $J(P_c)$ is connected if and only if the critical point 0 of P_c has bounded orbit. Moreover, they showed that there is a complete dichotomy of the parameter space of $\{P_c\}$: $J(P_c)$ is either connected (when $c \in M$) or totally disconnected ($c \in M^c$).

With Definition A, any c for which P_c has an attracting cycle other than ∞ lies in the Mandelbrot set M. A rational map is *hyperbolic* if every critical point of it is associated to an attracting cycle. It is conjectured that M is the topological closure of the set of hyperbolic parameters for P_c, which leads to Conjecture C.

To explain Proposition D, we recall (see e.g. Keen [8]) that given a map f_x in a parameterized family of holomorphic rational maps $\{f_\lambda\}$, the Julia set $J(f_x)$ *moves holomorphically* if for all x' in some neighborhood of x, f_x is quasiconformally conjugate to $f_{x'}$. The set of λ-values for which $J(f_\lambda)$ moves holomorphically is called the *J-stable set,* and its complement the *bifurcation locus.* The maps enjoy a type of structural stability as the parameter λ varies in a component of the J-stable set. For example, the number of attracting cycles and the period of each of them remain locally constant for maps corresponding to parameters in a component of the J-stable set (McMullen [11]). Mañé, Sad, and Sullivan [10] showed that the J-stable set is open and dense in the parameter space. The set of λ-values for which f_λ is hyperbolic forms an open and closed subset of the J-stable set ([11]). A component U is *hyperbolic* if for some parameter λ in U, and hence for all λ in U, f_λ is hyperbolic.

With Definition A, McMullen [11] proved that the boundary of the Mandelbrot set is the bifurcation locus of $\{P_c\}$, thus obtaining Proposition D. Moreover, he proved the following result.

Theorem 4.1 ([12])**.** *Quasiconformal copies of ∂M or a generalized version are dense in the bifurcation locus of any parameterized family of holomorphic rational maps.*

Now we compare $\{P_c\}$ and $\{R_a\}$. For $\{P_c\}$, each map has two critical points. The "pre-determined" critical point ∞ itself is a super-attracting fixed point. The Mandelbrot set M is defined as the set of c-values for which the orbit of the "free"

License or copyright restrictions may apply to redistribution; see https://www.ams.org/journal-terms-of-use

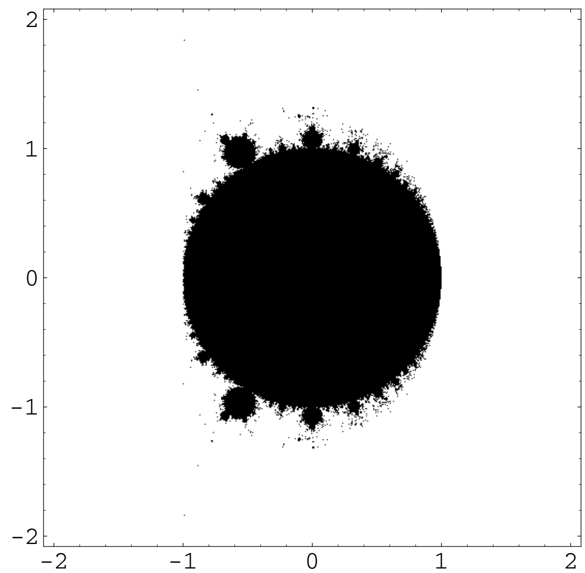

FIGURE 4. M'.

critical point 0 does not converge to the "pre-determined" critical point ∞: $M = \{c \in \mathbb{C} : {P_c}^n(0) \nrightarrow \infty\}$. Also, the parameter space of $\{P_c\}$ is already reduced; i.e., no two members of $\{P_c\}$ are conformally conjugate to each other.

As for $\{R_a\}$, each map has two distinct critical points c_1 and c_2. Assuming that c_1 is associated to the parabolic fixed point 0 for all parameters in the reduced set $\mathcal{R}_a$ (and thus assuming a stronger statement than Theorem 3.1), c_1 is the "pre-determined" critical point, and the behavior of the "free" critical point c_2 determines some features of $\mathcal{R}_a$. This shows similarities between the two families $\{P_c\}$ and $\{R_a\}$. We are interested in characterizing $\mathcal{R}_a$.

Definition (A). Define a set M' by $M' = \{a \in \mathcal{R}_a : {R_a}^n(c_2) \nrightarrow 0\}$.

The set M' is the set of a-values for which the orbit of the "free" critical point c_2 does not converge to the destination 0 of the orbit of the "pre-determined" critical point c_1. Figure 4 shows M' in $[-2, 2] \times [-2i, 2i]$.

The following results state that the reduced set $\mathcal{R}_a$ cannot be characterized as depicting the connectivity locus or hyperbolicity locus of $\{R_a\}$.

Theorem 4.2 ([16]). *If a quadratic rational map R has an invariant Fatou component containing two critical points, then the Julia set $J(R)$ is a Cantor set. Otherwise, $J(R)$ is connected.*

Corollary (B). *The Julia set $J(R_a)$ is connected for all $a \in \mathcal{R}_a$.*

Proof. Theorem 4.2 implies that the Julia set of a quadratic rational map R is either connected or totally disconnected. If $J(R)$ is totally disconnected, then its complement $F(R)$ is connected and consists of a single component. By construction R_a has a parabolic fixed point whose immediate basin consists of two disjoint Fatou components. Hence the Julia set $J(R_a)$ cannot be totally disconnected. Thus $J(R_a)$ is connected for all $a \in \mathcal{R}_a$. □

License or copyright restrictions may apply to redistribution; see https://www.ams.org/journal-terms-of-use

Proposition (C). *The map R_a is not hyperbolic for any $a \in \mathcal{R}_a$.*

Proof. By construction R_a always has a parabolic fixed point, and a critical point must be associated to it. Hence the map R_a is not hyperbolic for any $a \in \mathcal{R}_a$. □

Thus, describing the reduced set $\mathcal{R}_a$ as depicting the bifurcation locus of $\{R_a\}$ seems most appropriate.

Conjecture (D). *The bifurcation locus of $\{R_a\}$ is $\partial M'$.*

With Theorem 4.1 and Definition (A) we form the following conjecture.

Conjecture (E) (cf. [13])**.** *The bifurcation locus of $\{R_a\}$ is a quasiconformal image of the boundary of the Mandelbrot set without the period 2 limb.*

Appendix: Computer algorithm for drawing the parameter space of $\{R_a\}$

We explain the algorithm that produces the parameter space picture of $\{R_a\}$. The algorithm basically tracks critical orbits.

Computer algorithm for drawing the parameter space of $\{R_a\}$.

(i) Each pixel represents a parameter value a corresponding to the map R_a. Assign the default value 0 to each a.

(ii) For each a, we iterate the critical points $N > 0$ times to start. Let $s_i = {R_a}^N(c_i)$.

(iii) Choose $\epsilon > 0$ and set $M \in \mathbb{N}$ to be the maximal number of iterations. Apply the following test for each c_i: If the inequality $|{R_a}^n(s_i) - s_i| < \epsilon$ is satisfied in either the Euclidean metric or the spherical metric for some $n \in \mathbb{N}$, where $1 \leq n \leq M$, then we assign the value 1 to a.

(iv) Assign to each a the number of times the value 1 is assigned in (iii). Shade the parameters according to these numbers so that the parameters with the largest number are colored white and those with the smallest number are colored black.

The algorithm is supported by the following reasons. Generally speaking, if an attracting cycle has a multiplier of small modulus, then the iterates of the associated critical point(s) in the attracting immediate basin approach the points in the cycle quite quickly. This enables the inequality in (iii) to hold. Also, if a critical point is associated to a parabolic cycle, then although the attraction is very, very slow so that we may have to take many iterations (by letting N and n be large), the inequality in (iii) eventually holds. On the other hand, if a critical point is associated to a cycle of Siegel disks, then the image of the critical point after a finite number of iterations may not return near the critical point itself. This results in the inequality in (iii) being false for most $\epsilon > 0$ and most n.

References

[1] Baker, I.N. *Fixpoints of polynomials and rational functions.* J. London Math. Soc. 39 (1964), 615-622. MR0169989 (30:230)

[2] Beardon, A.F. *Iteration of Rational Functions.* Springer-Verlag, 1991. MR1128089 (92j:30026)

[3] Bergweiler, W. *On the number of critical points in parabolic basins.* Ergod. Th. & Dynam. Sys. 22 (2002), 655-669. MR1908548 (2003k:37059)

License or copyright restrictions may apply to redistribution; see https://www.ams.org/journal-terms-of-use

[4] Branner, B. *The Mandelbrot set*. In *Chaos and Fractals*, Proc. Sympos. Appl. Math. 39, pages 75-105. American Math. Soc., 1989. MR1010237

[5] Buff, X., and Epstein, A. *A parabolic Pommerenke-Levin-Yoccoz inequality*. Fundamenta Mathematicae 172 (2002), 249-289. MR1898687 (2003b:37067)

[6] Hagihara, R. *Rational Maps Lacking Certain Periodic Orbits*. PhD thesis, University of North Carolina at Chapel Hill, 2007.

[7] Hawkins, J. *Lebesgue ergodic rational maps in parameter space*. Int. J. Bifurcation and Chaos 13 (2003), no. 6, 1423-1447. MR1992056 (2004e:37065)

[8] Keen, L. *Julia sets of rational maps*. In *Complex Dynamical Systems: The Mathematics behind the Mandelbrot and Julia Sets*, Proc. Sympos. Appl. Math. 49, pages 71-89. American Math. Soc., 1994. MR1315534

[9] Kisaka, M. *On some exceptional rational maps*. Proc. Japan Acad., Ser. A 71 (1995), 35-38. MR1326795 (96a:30029)

[10] Mañé, R., Sad, P., and Sullivan, D. *On the dynamics of rational maps*. Ann. Scient. École Norm. Sup., 4^{e} série 16 (1983), 193-217. MR732343 (85j:58089)

[11] McMullen, C. *Complex Dynamics and Renormalization*. Annals of Math. Studies 135, Princeton Univ. Press, 1994. MR1312365 (96b:58097)

[12] McMullen, C. *The Mandelbrot set is universal*. In *The Mandelbrot Set, Theme and Variations*, London Math. Soc. Lecture Note Series 274, pages 1-17. Cambridge University Press, 2000. MR1765082 (2002f:37081)

[13] Milnor, J. *Geometry and dynamics of quadratic rational maps*. Experiment. Math. 2 (1993), no. 1, 37-83. MR1246482 (96b:58094)

[14] Milnor, J. *On rational maps with two critical points*. Experiment. Math. 9 (2000), no. 4, 481-522. MR1806289 (2001k:37074)

[15] Rees, M. *Components of degree two hyperbolic rational maps*. Invent. Math. 100 (1990), no. 2, 357-382. MR1047139 (91b:58187)

[16] Yin, Y.-C. *On the Julia sets of quadratic rational maps*. Compl. Variab. 18 (1992), 141-147. MR1157922 (93e:58160)

School of Mathematics and Statistics, University of New South Wales, Sydney, NSW 2052, Australia

E-mail address: `r.hagihara@unsw.edu.au`

License or copyright restrictions may apply to redistribution; see https://www.ams.org/journal-terms-of-use